Published in final edited form as:
J Neurosci. 2009 August 12; 29(32): 10104–10110. doi:10.1523/JNEUROSCI.2087-09.2009.

Glycinergic projection neurons of the cerebellum

Martha W. Bagnall[1,2], **Brian Zingg**[2], **Alexandra Sakatos**[2], **Setareh H. Moghadam**[2], **Hanns Ulrich Zeilhofer**[3,4], and **Sascha du Lac**[1,2,5]

[1]Neurosciences Graduate Program, University of California San Diego, La Jolla, California 92093
[2]Salk Institute for Biological Studies, 10010 N. Torrey Pines Rd., La Jolla, California 92037
[3]Institute of Pharmacology and Toxicology, University of Zurich, Winterthurerstrasse 190, CH-8057 Zurich, Switzerland [4]Institute of Pharmaceutical Sciences, ETH Zurich, Switzerland
[5]Howard Hughes Medical Institute

Abstract

The cerebellum funnels its entire output through a small number of presumed glutamatergic premotor projection neurons in the deep cerebellar nuclei and GABAergic neurons that feed back to the inferior olive. Here we use transgenic mice selectively expressing green fluorescent protein (GFP) in glycinergic neurons to demonstrate that many premotor output neurons in the medial cerebellar (fastigial) nuclei are in fact glycinergic, not glutamatergic as previously thought. These neurons exhibit similar firing properties as neighboring glutamatergic neurons and receive direct input from both Purkinje cells and excitatory fibers. Glycinergic fastigial neurons make functional projections to vestibular and reticular neurons in the ipsilateral brainstem, while their glutamatergic counterparts project contralaterally. Together these data suggest that the cerebellum can influence motor outputs via two distinct and complementary pathways.

Keywords

Cerebellum; Deep Cerebellar Nuclei; Glycine; Motor Control; Vestibular; Medulla

Introduction

Vertebrates rely on the cerebellum for precision timing, coordinated motion, and cognition (Kim et al., 1994; Spencer et al., 2003). Despite the diverse functions of the cerebellum, all Purkinje cell axons from cerebellar cortex converge on a comparatively small number of neurons in the deep cerebellar and vestibular nuclei. Two classes of projection neurons have been described in the deep cerebellar nuclei: GABAergic neurons which provide feedback signals to the inferior olive; and glutamatergic neurons which modulate premotor and cortical circuits via projections to the brainstem, midbrain, and thalamus. These large premotor neurons receive input from both mossy fibers and Purkinje cells and constitute the sole means by which the cerebellum influences behavior. In addition, the deep nuclei are thought to be a site of enduring cerebellar plasticity (Aizenman et al., 2000; Ohyama et al., 2006; Pugh and Raman, 2006; Thompson and Steinmetz, 2009). Thus it is critically important to understand how cerebellar nucleus neurons affect their downstream targets.

Although the literature refers exclusively to glutamatergic premotor (i.e., non-olivary) projection neurons of the deep cerebellar nuclei (Ito, 1984; Kandel et al., 1991; Squire et al.,

Correspondence: Dr. Sascha du Lac, sascha@salk.edu.

2008), histological reports indicate the presence of large deep nuclear neurons immunopositive for glycinergic markers (Chen and Hillman, 1993; Baurle and Grusser-Cornehls, 1997; Tanaka and Ezure, 2004; Chung et al., 2009). GABAergic neurons projecting to the inferior olive are small- to medium-sized, while local interneurons are thought to be small (Chan-Palay, 1977; de Zeeuw et al., 1989; Fredette and Mugnaini, 1991; Batini et al., 1992; De Zeeuw and Berrebi, 1995; Schwarz and Schmitz, 1997; Verveer et al., 1997; Teune et al., 1998; Uusisaari et al., 2007), raising the possibility that a subset of large projection neurons use glycine rather than glutamate as a neurotransmitter. Here we use a transgenic mouse line in which GFP is expressed under control of the GlyT2 (neuronal glycine transporter) promoter (Zeilhofer et al., 2005) to show that large glycinergic neurons in the fastigial nucleus are physiologically comparable to large glutamatergic projection neurons, are inhibited by Purkinje cells, and project outside the cerebellum to brainstem target regions.

Materials and Methods

Materials

Chemicals were from Sigma (St. Louis MO) unless otherwise specified. Rabbit anti-calbindin was diluted 1:200 (Chemicon, Temecula CA); Cy3 goat anti-rabbit (Chemicon) and Alexa 594 goat anti-rabbit (Molecular Probes, Invitrogen, Carlsbad CA) were diluted 1:100. Two transgenic mouse lines were used: the GlyT2-GFP line, in which glycinergic neurons are labeled with the fluorescent reporter GFP (Zeilhofer et al., 2005), and L7-tau-GFP, in which Purkinje cells are selectively labeled with GFP (Sekirnjak et al., 2003). All experiments were performed in accordance with the Salk Institute Animal Care and Use Committee rules.

Surgery

Animals were deeply anesthetized with isofluorane until breathing slowed to ~1 breath/s and the foot-pinch reflex vanished. They were then placed on a stereotaxic apparatus with a bite bar (Benchmark Angle Two, MyNeuroLab.com) and given continuous inhalation anesthesia as needed to maintain status. In most cases, a custom-made injector needle (0.2 mm OD, 0.1 mm ID, Creative Instruments Development Company; cidco@cox.net) was loaded with crystals of fluorolabeled dextran, either Texas Red, Cy3, or Cascade Blue, 10,000 MW (Molecular Probes) and the tip was sealed with melted bone wax. In other surgeries, dye was dissolved in water or DMSO and delivered with a pulled glass pipette. Stereotaxic coordinates were used to guide injections into the ventromedial and ventrolateral nuclei of the thalamus (n = 5) and the lateral vestibular nucleus (n = 2). For medullary injections (n = 4), the midline was visually identified after blunt dissection of the neck muscles and fiber tracts were targeted unilaterally ~0.3mm lateral to the midline, with a needle depth of 1.25 mm. After the needle was lowered, the interior plunger was repeatedly depressed (~100 μm) with calibrated air pressure (25 psi, 25 ms) to deliver the crystals into the tissue. After waiting 1–2 min for the dye to settle, the needle was withdrawn and the skin sutured. Animals were treated post-surgery with Buprenex (1.5 μg in saline) to minimize discomfort. 4–8 days after injection, mice were sacrificed.

Tissue preparation

Adult animals (> P28; typically 2–5 months old) from both GlyT2-GFP and L7-GFP mouse lines were anesthetized with Nembutal and perfused transcardially with phosphate-buffered saline (PBS) followed by 4% paraformaldehyde in PBS (PFA) for 5 min. After removal of the brain from the skull, the tissue was post-fixed for 30–60 min in PFA, then sunk in 30% sucrose in PBS overnight at 4 °C. 20–50 μm coronal or sagittal sections were cut on a freezing microtome (Microm) and washed in PBS or in some cases mounted directly onto

slides. For immunocytochemistry of free floating sections, blocking buffer (2% normal goat serum, 1% bovine serum albumin, and 0.3% Triton X-100 in PBS) was applied for 1 hr, followed by primary antibody in working buffer (10-fold dilution of blocking buffer) overnight at 4 °C. Sections were washed 3 times with working buffer and treated with fluoro-conjugated secondary antibody for 1 hr at room temperature. Following washes in PBS, sections were wet-mounted and coverslipped with 2.5% DABCO or Vectashield Hardset (Vector Labs, Burlingame CA).

For electron microscopic analyses, the paraformaldehyde-fixed brain of a 2 month old (P50) GlyT2-GFP mouse was rinsed in cold PBS and the cerebellum was cut into 50 μm slices on a vibratome. Slices were imaged on a fluorescence microscope to locate large GFP-expressing neurons in the fastigial nucleus. Slices were then post-fixed in 2% glutaraldehyde in 0.1M sodium cacodylate buffer, rinsed, postfixed in 1% osmium tetroxide and 1% potassium ferrocyanide, rinsed, en bloc stained in 1% uranyl acetate, dehydrated with glycol methacrylate and flat embedded in Epon. The slices were blocked and mounted onto Epon stubs. Ultrathin sections (~60 nm) were cut on an ultramicrotome, collected onto formvar-coated slot grids and stained with 2% uranyl acetate and 0.2% lead citrate. The sections were examined in a JEOL 100CXII transmission electron microscope equipped with a digital camera. All chemicals were acquired from Electron Microscopy Sciences (Fort Washington PA).

Image acquisition and processing

Epifluorescent images were recorded using a Hamamatsu CCD camera attached to a Olympus BX60 or BX61 light microscope with a 4× (NA 0.13) or 10× (NA 0.3) objective lens with SlideBook 4. Confocal images were acquired in 0.1 – 0.5 μm steps on a Leica TCS SP2 AOBS microscope using laser lines of 488 and 561 nm, with a 20× (NA 0.5) or 63× (NA 1.4) objective and in some cases 3× hardware zoom. In most cases images were collected by sequential scanning to avoid possible fluorophore crosstalk. Leica software was used to average sequential z-planes in images (2–6 z-planes representing < 3 μm total). Images were transferred to Adobe Photoshop for whole-image brightness/contrast adjustment and image overlay.

Coronal cerebellar sections from three GlyT2-GFP mice were used for sizing analysis. Two of these contained retrogradely labeled neurons from dye injections in either the vestibular nuclei or the caudal medulla. Confocal images were acquired in 1 μm steps with a 40× objective. Neuronal area and maximum diameter were assessed using Neurolucida. Non-projecting neurons were randomly selected from the fastigial, interpositus, and dentate nuclei; retrogradely labeled neurons were identified in the fastigial nuclei. Throughout this paper, for ease of reference to the homologous nuclei in primates, we use the terms “fastigial, interpositus, and dentate” to refer to the medial, interposed, and lateral cerebellar nuclei, respectively.

Electrophysiology and reverse transcription PCR

Coronal cerebellar slices were cut from GlyT2-GFP mice aged P10–14; dense myelination in the deep nuclei and lateral vestibular nuclei in older animals is prohibitive for routine patch-clamp recording. Recordings were made at ~33°C using a combination of epifluorescence and infrared illumination with differential interference contrast to visualize neurons. Data were collected and analyzed with custom-written code in Igor Pro 5. Ringer’s solution for slicing and recording consisted of (in mM): 124 NaCl, 26 $NaHCO_3$, 5 KCl, 1.3 MgCl, 1 NaH_2PO_4, 11 dextrose. Pipette internal solution: 140 K-gluconate, 10 HEPES, 8 NaCl, 0.1 EGTA, 2 MgATP, 0.3 Na_2GTP. In experiments examining synaptic projections, the following receptor antagonists were present as noted: 6,7-dinitroquinoxaline-2,3-dione

(DNQX, 10 μM) to block fast ionotropic glutamatergic transmission, D-aminophosphonovaleric acid (D-APV, 25 μM) or R-3-(2carboxypiperazin-4-yl)propyl-1-phosphonic acid (R-CPP, 25 μM, Ascent Scientific) to block N-methyl-D-aspartate receptor-mediated transmission, strychnine (1 μM) to block glycine receptors, gabazine (SR95531; 10 μM) to block ionotropic GABAergic receptors. All synaptic data were acquired in the presence of these antagonists, with the appropriate blocker washed in at the experiment's conclusion to verify transmitter identity. Latency is reported as the time to 10% of the peak IPSC. For excitatory inputs, neurons were clamped at ~−75 to −80 mV; for inhibitory inputs, at −60 to −50 mV (junction potential corrected). Data are reported as means ± SEM unless otherwise noted. Single-cell RT-PCR was carried out as described previously (Bagnall et al., 2007) using primers to VGluT1, VGluT2, and GlyT2.

Statistics

Nonparametric statistics were used for all analyses of intrinsic physiological data. The Kruskal-Wallis test was used to determine multiple group comparison validity, followed by the Wilcoxon unpaired test for between-group comparisons. Kruskal-Wallis values were as follows: maximum firing rate, 0.0029; input resistance, 0.00019; spike width, <0.0001. Synaptic responses to trains are presented as means ± S.E.M. Cell size comparisons are presented as means ± S.D.

Results

We identified glycinergic neurons in cerebellar tissue with a recently developed transgenic mouse line in which GFP is expressed under the promoter for the neuronal glycine transporter GlyT2 (Zeilhofer et al., 2005) (Fig 1a). Many GlyT2-GFP+ neurons in the rostral two-thirds of the fastigial nucleus, concentrated ventrally, were ~20 μm in diameter (Fig 1b), comparable in size to the large projection neurons found in all three deep nuclei (Chan-Palay, 1977). Unilaterally these neurons numbered ~280, or approximately 15% of all large fastigial neurons (Heckroth, 1994) (GlyT2-GFP fastigial image series, Supplemental Fig. 1). In contrast, GFP+ neurons in the interpositus and dentate deep nuclei were smaller, on average ~12 μm in diameter, indicating likely local interneurons (Fig. 1c) ((Chan-Palay, 1977; Chen and Hillman, 1993); see also Fig. 4d and associated text).

To verify the accuracy of GFP expression, single neurons from the fastigial nuclei were subjected to reverse transcription PCR for three neurotransmitter markers (Bagnall et al., 2007): the vesicular glutamate transporters VGluT1 and VGluT2, and GlyT2. Large GFP+ neurons expressed GlyT2, but neither VGluT1 nor VGluT2 (n = 7). In contrast, large GFP– neurons contained VGluT2, but not VGluT1 or GlyT2 (Fig. 1d, n = 4). Thus although the majority of large fastigial neurons are, as expected, glutamatergic, the GlyT2-GFP transgenic line appropriately identifies a distinct set of large glycinergic neurons. To identify the role that these neurons play in the cerebellar circuit, we tested in turn the synaptic inputs and intrinsic processing properties of large Gly+ neurons.

Deep nuclear projection neurons receive two major types of input: dense GABAergic input from Purkinje cells in the cerebellar cortex, and glutamatergic input primarily from mossy fiber collaterals. Purkinje cell innervation was assessed at the light microscopic level using immunostaining for calbindin D-28k, which colocalizes with Purkinje cell terminals (Batini, 1990) as identified in the L7-tau-GFP transgenic mouse line, in which Purkinje cells selectively express GFP (Sekirnjak et al., 2003) (Fig. 2a). Calbindin immunostaining in GlyT2-GFP mice revealed that large fastigial glycinergic somata were surrounded by numerous Purkinje cell synaptic terminals, similar to the known innervation pattern in projection but not intrinsic neurons (Chan-Palay, 1977; Uusisaari and Knopfel, 2008) (Fig. 2b). At the ultrastructural level, Purkinje cell terminals are recognizable by their large size,

flattened vesicles, and multiple release sites (Chan-Palay, 1977; Telgkamp et al., 2004). Electron microscopy revealed the presence of many such axon terminals surrounding the soma of large glycinergic neurons (Fig. 2c). These boutons contained multiple symmetric synapses and flattened vesicles typical of Purkinje cell GABAergic synapses (Fig. 2d).

Purkinje cell synapses exhibit several distinctive physiological characteristics, including sustained transmission at high frequencies (Telgkamp and Raman, 2002; Telgkamp et al., 2004). We made voltage clamp recordings from large glycinergic neurons in slice preparation while stimulating the cerebellar vermis, the source of most Purkinje cell input to fastigial neurons. The resulting gabazine-sensitive synaptic current (example, Fig. 2e) was robust even at high frequencies of stimulation (Fig. 2f, n = 4), consistent with Purkinje cell synaptic characteristics (Telgkamp and Raman, 2002; Telgkamp et al., 2004). Thus not all large Purkinje cell recipient neurons in the deep nuclei are glutamatergic, as had previously been thought (Chan-Palay, 1977; Batini et al., 1992; De Zeeuw and Berrebi, 1995; Teune et al., 1998).

Synaptic stimulation in the presence of blockers of ionotropic inhibitory transmission evoked fast inward currents that were abolished by application of glutamatergic receptor antagonists (example, Fig. 2g). These inputs presumably represent mossy fiber collaterals, which make excitatory synapses onto deep nuclear neurons; at the ultrastructural level, some synaptic terminals with typical excitatory characteristics (clear round vesicles, asymmetric synaptic densities) were also visible (data not shown). Therefore, large glycinergic neurons in the deep nuclei receive the same fundamental forms of circuit information as glutamatergic neurons.

In most systems, projection and local neurons exhibit different intrinsic physiological characteristics suited to their circuit function. Projection neurons and interneurons in the deep cerebellar nuclei also differ in several essential features, including firing rate and action potential waveform (Jahnsen, 1986; Aizenman et al., 2003; Uusisaari et al., 2007). To determine whether large Gly+ neurons more closely resemble their large excitatory or small inhibitory neighbors, we made recordings of all three types of neurons in cerebellar slices. Action potentials of both large glycinergic and glutamatergic neurons were less than half as broad as those of small glycinergic neurons (Fig. 3a, c). In response to a 1 s depolarizing current step, both Gly+ and Gly– large neurons were capable of firing action potentials at rates ranging from ~100 to 450 spikes/s, while maximum firing rates of Gly+ small neurons saturated < 120 spikes/s (Fig. 3b, c). In addition, subthreshold input resistance was significantly higher in small neurons than in either group of large neurons (Fig. 3c). Thus the intrinsic properties of large glycinergic neurons are indistinguishable from those of large glutamatergic neurons, but distinct from those of small glycinergic presumed interneurons. Notably, large Gly+ neurons are also physiologically dissimilar from deep nuclear GABAergic neurons, in which action potentials are wider and firing saturates at ~50 spikes/s at room temperature (Uusisaari et al., 2007). Do large glycinergic neurons function as local cerebellar interneurons of unusual girth, or as premotor projection neurons, like the large glutamatergic neurons they resemble physiologically?

To evaluate whether Gly+ fastigial neurons project to other brain areas, fluorescently-conjugated dextrans were injected into target regions to label via retrograde transport any neurons projecting to or through the site of injection. Following dye injection to the caudal ventral medulla, which labels axons projecting to the medullary reticular nuclei and spinal cord (Fig. 4a), confocal fluorescence microscopy revealed retrogradely labeled fastigial neurons in both halves of the fastigial nuclei, as expected (Matsushita and Hosoya, 1978; Asanuma et al., 1983). Interestingly, labeled fastigial neurons ipsilateral to the injection site were glycinergic (Fig. 4b), while those contralateral were glutamatergic (Fig. 4c) and

segregated spatially in the dorsal half of the nucleus. Retrogradely labeled Gly+ neurons from injections into the reticular formation or lateral vestibular nucleus were significantly larger than the population of Gly+ neurons as a whole (long × short diameters: Gly+ projection neurons, 189 ± 67.5 μm^2 [s.d.]; all Gly+ neurons, 132 ± 75.6; $p < 0.0001$, unpaired t-test), supporting the conclusion that large Gly+ neurons make extracerebellar projections, while small Gly+ neurons serve as local interneurons (Fig. 4d).

To localize specific targets of glycinergic outputs, we made unilateral dye injections directly into the fastigial nucleus. Glycinergic efferents traveled caudally in the ventral brainstem to the ipsilateral ventromedial medullary reticular formation (Asanuma et al., 1983; Homma et al., 1995), where they issued terminal boutons that contacted both glycinergic and non-glycinergic neurons (Fig. 4e, f). Glycinergic efferents could also be followed to the ipsilateral lateral and descending vestibular nuclei (Fig. 4g), known targets of fastigial output (Homma et al., 1995). Dye injections into these target regions also resulted in retrograde labeling of ipsilateral glycinergic and contralateral glutamatergic fastigial neurons (data not shown). In contrast, thalamic tracer injection produced exclusively glutamatergic labeling of neurons that were concentrated in the caudal one-third of the contralateral fastigial nucleus (Fig. 4h), consistent with data from other species (Angaut and Bowsher, 1970; Sugimoto et al., 1981; Noda et al., 1990; Teune et al., 2000). Thus it appears that fastigial glycinergic outputs are segregated to brainstem and caudal targets and do not extend rostrally.

To determine whether fastigial neurons identified in the GlyT2 transgenic mouse line actually release glycine onto their postsynaptic targets, we pursued physiological analysis of the fastigio-vestibular pathway. Thick coronal slices (~450 μm) from juvenile animals were used to maintain the fastigial nucleus, a section of cerebellar peduncle, and the lateral vestibular nucleus in one preparation (Fig. 5a). Whole-cell recordings were made from vestibular nucleus neurons while stimulating the fastigial nucleus in the presence of blockers of ionotropic glutamatergic and GABAergic synaptic transmission. The resulting outward synaptic current had a median latency of 1.5 ms and was fully blocked by the glycine receptor antagonist strychnine (1 μM; n = 6) (example, Fig. 5b). Application of 50-Hz stimulus trains consistently drove synaptic facilitation followed by sustained transmission (Fig. 5c, d; n = 5). Together these data demonstrate a functional, ipsilateral glycinergic synaptic projection from the medial cerebellar nucleus to the brainstem.

Discussion

The cerebellum has been traditionally thought to influence the rest of the brain via two types of pathways emanating from the deep nuclei: a GABAergic feedback loop to the inferior olive, and a glutamatergic projection to diverse brain regions. Our findings demonstrate the presence of a third, glycinergic pathway from the fastigial nucleus to the ipsilateral brainstem. It is matched by contralateral glutamatergic projections to the same vestibular and medullary reticular nuclei, providing a means for the cerebellum to coordinate midline musculature subserving balance and postural movements. Glycinergic and glutamatergic projection neurons are indistinguishable at the level of synaptic inputs and intrinsic physiology, indicating a common information processing scheme for excitatory and inhibitory premotor cerebellar nuclear neurons.

The fastigial nucleus has been divided into two functionally distinct parts that differ in neuronal response properties and projections (Ito, 1984; Thach et al., 1992). Rostral fastigial neurons are thought to mediate adaptive control of balance, posture, and autonomic function via their projections to brainstem vestibular and reticular nuclei. In contrast, caudal fastigial neurons are involved in cortical function and oculomotor control and project to the thalamus

and to eye movement related portions of the brainstem and midbrain nuclei (Batton et al., 1977; Noda et al., 1990; Buttner et al., 1991). Their rostral location and postsynaptic targets in the vestibular nuclei and caudal brainstem implicate fastigial glycinergic projection neurons in balance and postural control.

Although the majority of deep cerebellar nucleus neurons project contralaterally, studies in a variety of species have demonstrated a prominent projection from the fastigial nucleus to the ipsilateral lateral and descending vestibular nuclei as well as a more modest projection to the ipsilateral medullary reticular formation (Ito, 1984). Our data confirm the presence of these pathways in mouse and identify the scattering of large glycinergic neurons observed in previous studies (Chen and Hillman, 1993; Baurle and Grusser-Cornehls, 1997; Tanaka and Ezure, 2004; Chung et al., 2009) as the major source of these ipsilateral projections. Inactivation of the rostral fastigal nucleus results in a tendency to fall toward the side of inactivation (Thach et al., 1992; Kurzan et al., 1993; Pelisson et al., 1998), as expected from a fastigial projection pattern of ipsilateral inhibition and contralateral excitation.

Why are glycinergic projection neurons found in the fastigial nucleus but not the interpositus and dentate? The parallel glycinergic and glutamatergic ouput channels of the rostral fastigial are well suited for directing behaviors that rely on cross-midline coordination, such as postural adjustments and gait. Interestingly, the vestibular control of horizontal eye movements is accomplished via ipsilateral glycinergic and contralateral glutamatergic outputs from the medial vestibular nucleus to the abducens ocular motor nuclei (Ito et al., 1977; Spencer et al., 1989). We hypothesize that during the evolutionary development of the fastigial nucleus, some of the horizontal vestibular bauplan was retained for coordination of midline musculature. In contrast, the later-evolving interpositus and dentate nuclei, which are critical for control of axial musculature, rely exclusively on glutamatergic premotor projections.

Several lines of evidence now demonstrate that the functional circuitry of the cerebellum, despite its crystalline architecture, is not homogeneous. Parasagittal zones defined by the enzymatic marker zebrin II (aldolase C) (Leclerc et al., 1992) differ in expression of proteins and their subnuclear target localization (Sugihara and Shinoda, 2007), synaptic transmission parameters, and plasticity rules (Wadiche and Jahr, 2005). One type of excitatory interneuron, the unipolar brush cell, resides exclusively in the vestibulo-cerebellum (Dugue et al., 2005; Diana et al., 2007). Our findings indicate that premotor circuit connectivity differs across cerebellar nuclei, and that the midline fastigial nucleus contains both glutamatergic and glycinergic output channels.

The evidence presented here demonstrates that glycinergic and glutamatergic projection neurons in the fastigial nuclei share an essential role in the cerebellar circuit. They are indistinguishable in their intrinsic properties, but physiologically distinct from small local glycinergic neurons, indicating that circuit role, rather than transmitter content per se, influences their processing properties, as has been shown for the medial vestibular nucleus (Bagnall et al., 2007).

Notably, all components of the cerebellar motor control circuit operate around high baseline firing rates. Both excitatory and inhibitory inputs to projection neurons are capable of sustaining high frequency synaptic transmission (Fig. 2) (Telgkamp and Raman, 2002; Telgkamp et al., 2004). *In vivo*, rostral fastigial neurons fire spontaneously at 30–60 Hz (Buttner et al., 1991; Miller et al., 2008), and both glycinergic and glutamatergic projection neurons can maintain high firing rates *in vitro* (Fig. 3). We provide the first evidence, to the best of our knowledge, that deep nuclear neurons evoke reliable synaptic currents that exhibit sustained transmission at physiological rates of activity (Fig. 5). Whether or not

excitatory outputs from the deep nuclei exhibit similar properties remains to be determined (Gorodnov and Fanardjian, 1987; Jiang et al., 2002). Thus, rapid ongoing activity is a hallmark of cerebellar motor control and may be critical for fast, temporally precise modulation of movement.

Because the properties of glycinergic and glutamatergic neurons are so similar, it is likely that glycinergic and glutamatergic projection neurons are difficult to differentiate during *in vivo* experiments unless their precise projections are known; thus much of the literature on fastigial activity likely includes data from both types of neurons. It is known that an individual Purkinje cell can make synaptic contacts onto both glutamatergic and GABAergic neurons (De Zeeuw and Berrebi, 1995). If the same is true for divergence onto both glutamatergic and glycinergic projection neurons, then a single Purkinje cell could influence coordinated bilateral movement by affecting both ipsilateral and contralateral premotor structures.

Supplementary Material

Refer to Web version on PubMed Central for supplementary material.

Acknowledgments

This work was supported by the Howard Hughes Medical Institute and National Institute of Health EY-11027 to S.d.L., and a National Science Foundation Graduate Research Fellowship to M.W.B. We thank Richard Jacobs for electron microscopy.

References

Aizenman CD, Huang EJ, Linden DJ. Morphological correlates of intrinsic electrical excitability in neurons of the deep cerebellar nuclei. J Neurophysiol. 2003; 89:1738–1747. [PubMed: 12686564]

Aizenman CD, Huang EJ, Manis PB, Linden DJ. Use-dependent changes in synaptic strength at the Purkinje cell to deep nuclear synapse. Prog Brain Res. 2000; 124:257–273. [PubMed: 10943131]

Angaut P, Bowsher D. Ascending projections of the medial cerebellar (fastigial) nucleus: an experimental study in the cat. Brain Res. 1970; 24:49–68. [PubMed: 5503234]

Asanuma C, Thach WT, Jones EG. Brainstem and spinal projections of the deep cerebellar nuclei in the monkey, with observations on the brainstem projections of the dorsal column nuclei. Brain Res. 286:299–322.

Bagnall MW, Stevens RJ, du Lac S. Transgenic mouse lines subdivide medial vestibular nucleus neurons into discrete, neurochemically distinct populations. J Neurosci. 2007; 27:2318–2330. [PubMed: 17329429]

Batini C. Cerebellar localization and colocalization of GABA and calcium binding protein-D28K. Arch Ital Biol. 1990; 128:127–149. [PubMed: 2268180]

Batini C, Compoint C, Buisseret-Delmas C, Daniel H, Guegan M. Cerebellar nuclei and the nucleocortical projections in the rat: retrograde tracing coupled to GABA and glutamate immunohistochemistry. J Comp Neurol. 1992; 315:74–84. [PubMed: 1371781]

Batton RR, Jayaraman A, Ruggiero D, Carpenter MB. Fastigial efferent projections in the monkey: an autoradiographic study. J Comp Neurol. 1977; 174:281–305. [PubMed: 68041]

Baurle J, Grusser-Cornehls U. Differential number of glycine- and GABA-immunopositive neurons and terminals in the deep cerebellar nuclei of normal and Purkinje cell degeneration mutant mice. J Comp Neurol. 1997; 382:443–458. [PubMed: 9184992]

Buttner U, Fuchs AF, Markert-Schwab G, Buckmaster P. Fastigial nucleus activity in the alert monkey during slow eye and head movements. J Neurophysiol. 1991; 65:1360–1371. [PubMed: 1875245]

Chan-Palay, V. Cerebellar Dentate Nucleus: Organization, Cytology and Transmitters. Berlin: Springer-Verlag; 1977.

Chen S, Hillman DE. Colocalization of neurotransmitters in the deep cerebellar nuclei. J Neurocytol. 1993; 22:81–91. [PubMed: 8095297]

Chung S-H, Marzban H, Hawkes R. Compartmentalization of the cerebellar nuclei of the mouse. Neuroscience. 2009

De Zeeuw CI, Berrebi AS. Postsynaptic targets of Purkinje cell terminals in the cerebellar and vestibular nuclei of the rat. Eur J Neurosci. 1995; 7:2322–2333. [PubMed: 8563981]

de Zeeuw CI, Holstege JC, Ruigrok TJ, Voogd J. Ultrastructural study of the GABAergic, cerebellar, and mesodiencephalic innervation of the cat medial accessory olive: anterograde tracing combined with immunocytochemistry. J Comp Neurol. 1989; 284:12–35. [PubMed: 2474000]

Diana MA, Otsu Y, Maton G, Collin T, Chat M, Dieudonne S. T-type and L-type Ca2+ conductances define and encode the bimodal firing pattern of vestibulocerebellar unipolar brush cells. J Neurosci. 2007; 27:3823–3838. [PubMed: 17409247]

Dugue GP, Dumoulin A, Triller A, Dieudonne S. Target-dependent use of coreleased inhibitory transmitters at central synapses. J Neurosci. 2005; 25:6490–6498. [PubMed: 16014710]

Fredette BJ, Mugnaini E. The GABAergic cerebello-olivary projection in the rat. Anat Embryol. 1991; 184:225–243. [PubMed: 1793166]

Gorodnov VL, Fanardjian VV. Functional properties of the cerebellorubral synapses in the cat. Brain Res. 1987; 410:340–342. [PubMed: 3036310]

Heckroth JA. Quantitative morphological analysis of the cerebellar nuclei in normal and lurcher mutant mice. I. Morphology and cell number. J Comp Neurol. 1994; 343:173–182. [PubMed: 8027434]

Homma Y, Nonaka S, Matsuyama K, Mori S. Fastigiofugal projection to the brainstem nuclei in the cat: an anterograde PHA-L tracing study. Neurosci Res. 1995; 23:89–102. [PubMed: 7501304]

Ito, M. The cerebellum and neural control. New York: Raven Press; 1984.

Ito M, Nisimaru N, Yamamoto M. Specific patterns of neuronal connexions involved in the control of the rabbit's vestibulo-ocular reflexes by the cerebellar flocculus. J Physiol. 1977; 265:833–854. [PubMed: 300801]

Jahnsen H. Electrophysiological characteristics of neurones in the guinea-pig deep cerebellar nuclei in vitro. J Physiol. 1986; 372:129–147. [PubMed: 3723407]

Jiang MC, Alheid GF, Nunzi MG, Houk JC. Cerebellar input to magnocellular neurons in the red nucleus of the mouse: synaptic analysis in horizontal brain slices incorporating cerebello-rubral pathways. Neuroscience. 2002; 110:105–121. [PubMed: 11882376]

Kandel, ER.; Schwartz, JH.; Jessell, TM. Principles of Neural Science. 3 Edition. Norwalk, Connecticut: Appleton & Lange; 1991.

Kim SG, Ugurbil K, Strick PL. Activation of a cerebellar output nucleus during cognitive processing. Science. 1994; 265:949–951. [PubMed: 8052851]

Kurzan R, Straube A, Buttner U. The effect of muscimol micro-injections into the fastigial nucleus on the optokinetic response and the vestibulo-ocular reflex in the alert monkey. Exp Brain Res. 1993; 94:252–260. [PubMed: 8359241]

Leclerc N, Schwarting GA, Herrup K, Hawkes R, Yamamoto M. Compartmentation in mammalian cerebellum: Zebrin II and P-path antibodies define three classes of sagittally organized bands of Purkinje cells. Proc Natl Acad Sci U S A. 1992; 89:5006–5010. [PubMed: 1594607]

Matsushita M, Hosoya Y. The location of spinal projection neurons in the cerebellar nuclei (cerebellospinal tract neurons) of the cat. A study with the horseradish peroxidase technique. Brain Res. 1978; 142:237–248. [PubMed: 630384]

Miller DM, Cotter LA, Gandhi NJ, Schor RH, Huff NO, Raj SG, Shulman JA, Yates BJ. Responses of rostral fastigial nucleus neurons of conscious cats to rotations in vertical planes. Neuroscience. 2008; 155:317–325. [PubMed: 18571332]

Noda H, Sugita S, Ikeda Y. Afferent and efferent connections of the oculomotor region of the fastigial nucleus in the macaque monkey. J Comp Neurol. 1990; 302:330–348. [PubMed: 1705268]

Ohyama T, Nores WL, Medina JF, Riusech FA, Mauk MD. Learning-induced plasticity in deep cerebellar nucleus. J Neurosci. 2006; 26:12656–12663. [PubMed: 17151268]

Pelisson D, Goffart L, Guillaume A. Contribution of the rostral fastigial nucleus to the control of orienting gaze shifts in the head-unrestrained cat. J Neurophysiol. 1998; 80:1180–1196. [PubMed: 9744931]

Pugh JR, Raman IM. Potentiation of mossy fiber EPSCs in the cerebellar nuclei by NMDA receptor activation followed by postinhibitory rebound current. Neuron. 2006; 51:113–123. [PubMed: 16815336]

Schwarz C, Schmitz Y. Projection from the cerebellar lateral nucleus to precerebellar nuclei in the mossy fiber pathway is glutamatergic: a study combining anterograde tracing with immunogold labeling in the rat. J Comp Neurol. 1997; 381:320–334. [PubMed: 9133571]

Sekirnjak C, Vissel B, Bollinger J, Faulstich M, du Lac S. Purkinje cell synapses target physiologically unique brainstem neurons. J Neurosci. 2003; 23:6392–6398. [PubMed: 12867525]

Spencer RF, Wenthold RJ, Baker R. Evidence for glycine as an inhibitory neurotransmitter of vestibular, reticular, and prepositus hypoglossi neurons that project to the cat abducens nucleus. J Neurosci. 1989; 9:2718–2736. [PubMed: 2570136]

Spencer RM, Zelaznik HN, Diedrichsen J, Ivry RB. Disrupted timing of discontinuous but not continuous movements by cerebellar lesions. Science. 2003; 300:1437–1439. [PubMed: 12775842]

Squire, LR.; Bloom, FE.; Spitzer, NC.; du Lac, S.; Ghosh, A.; Berg, D. Fundamental Neuroscience. San Diego: Academic Press; 2008.

Sugihara I, Shinoda Y. Molecular, topographic, and functional organization of the cerebellar nuclei: analysis by three-dimensional mapping of the olivonuclear projection and aldolase C labeling. J Neurosci. 2007; 27:9696–9710. [PubMed: 17804630]

Sugimoto T, Mizuno N, Itoh K. An autoradiographic study on the terminal distribution of cerebellothalamic fibers in the cat. Brain Res. 1981; 215:29–47. [PubMed: 6167316]

Tanaka I, Ezure K. Overall distribution of GLYT2 mRNA-containing versus GAD67 mRNA-containing neurons and colocalization of both mRNAs in midbrain, pons, and cerebellum in rats. Neurosci Res. 2004; 49:165–178. [PubMed: 15140559]

Telgkamp P, Raman IM. Depression of inhibitory synaptic transmission between Purkinje cells and neurons of the cerebellar nuclei. J Neurosci. 2002; 22:8447–8457. [PubMed: 12351719]

Telgkamp P, Padgett DE, Ledoux VA, Woolley CS, Raman IM. Maintenance of high-frequency transmission at purkinje to cerebellar nuclear synapses by spillover from boutons with multiple release sites. Neuron. 2004; 41:113–126. [PubMed: 14715139]

Teune TM, van der Burg J, De Zeeuw CI, Voogd J, Ruigrok TJ. Single Purkinje cell can innervate multiple classes of projection neurons in the cerebellar nuclei of the rat: a light microscopic and ultrastructural triple-tracer study in the rat. J Comp Neurol. 1998; 392:164–178. [PubMed: 9512267]

Teune TM, van der Burg J, van der Moer J, Voogd J, Ruigrok TJ. Topography of cerebellar nuclear projections to the brain stem in the rat. Prog Brain Res. 2000; 124:141–172. [PubMed: 10943123]

Thach WT, Goodkin HP, Keating JG. The cerebellum and the adaptive coordination of movement. Annu Rev Neurosci. 1992; 15:403–442. [PubMed: 1575449]

Thompson RF, Steinmetz JE. The Role of the Cerebellum in Classical Conditioning of Discrete Behavioral Responses. Neuroscience. 2009

Uusisaari M, Knopfel T. GABAergic synaptic communication in the GABAergic and non-GABAergic cells in the deep cerebellar nuclei. Neuroscience. 2008; 156:537–549. [PubMed: 18755250]

Uusisaari M, Obata K, Knopfel T. Morphological and electrophysiological properties of GABAergic and non-GABAergic cells in the deep cerebellar nuclei. J Neurophysiol. 2007; 97:901–911. [PubMed: 17093116]

Verveer C, Hawkins RK, Ruigrok TJ, De Zeeuw CI. Ultrastructural study of the GABAergic and cerebellar input to the nucleus reticularis tegmenti pontis. Brain Res. 1997; 766:289–296. [PubMed: 9359619]

Wadiche JI, Jahr CE. Patterned expression of Purkinje cell glutamate transporters controls synaptic plasticity. Nat Neurosci. 2005; 8:1329–1334. [PubMed: 16136036]

Zeilhofer HU, Studler B, Arabadzisz D, Schweizer C, Ahmadi S, Layh B, Bosl MR, Fritschy JM. Glycinergic neurons expressing enhanced green fluorescent protein in bacterial artificial chromosome transgenic mice. J Comp Neurol. 2005; 482:123–141. [PubMed: 15611994]

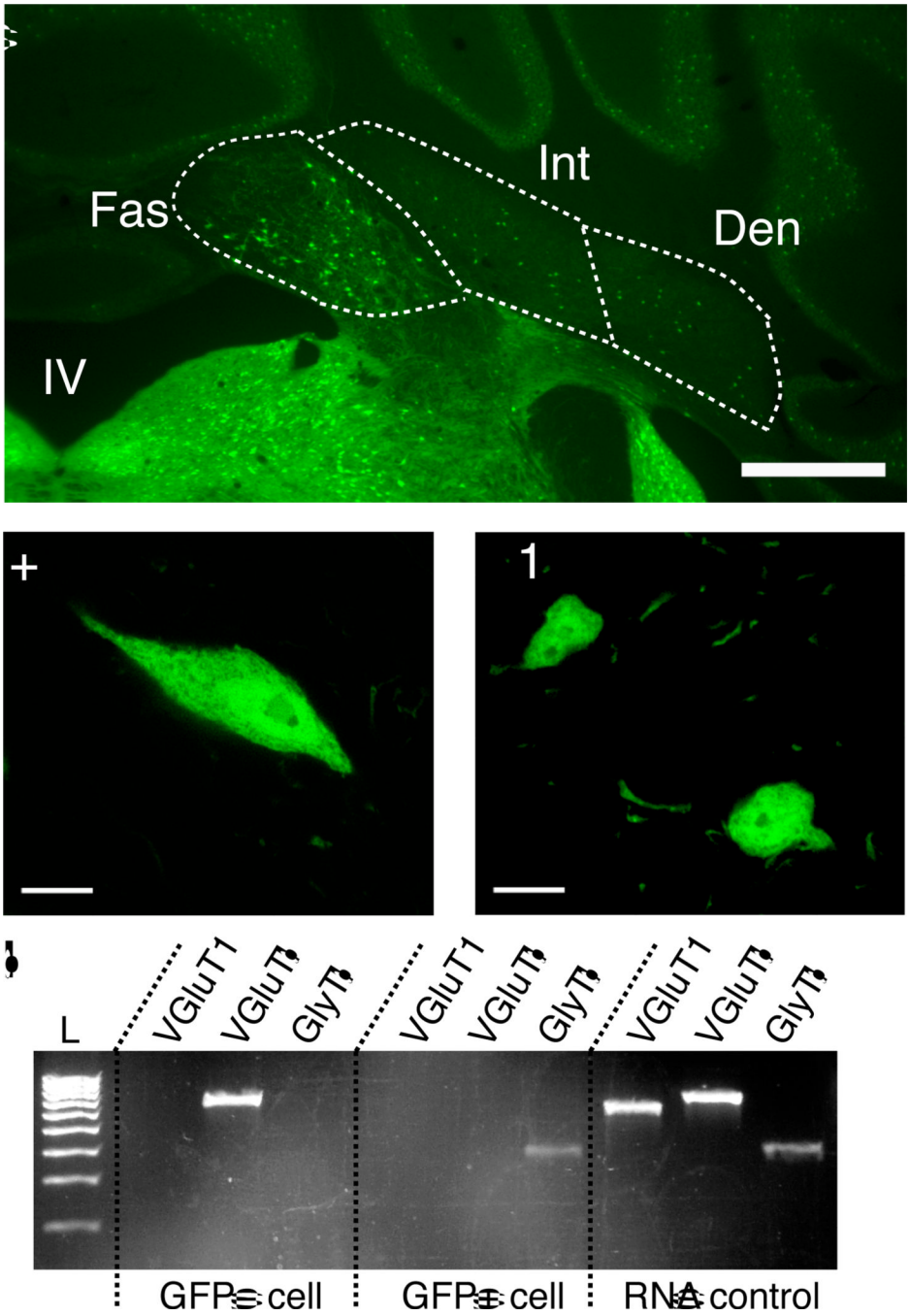

Figure 1. Identification of large glycinergic neurons in the fastigial nuclei

a) Coronal section of cerebellum and brainstem in the GlyT2-GFP mouse. Large GFP+ cells are evident in the fastigial (Fas), but not the interpositus (Int) or dentate (Den) deep cerebellar nuclei. Scattered cerebellar Golgi cells are also visible. IV, 4th ventricle. Scale bar, 500μm. **b)** Confocal image of a large fastigial GFP+ neuron, and **c)** small dentate GFP+ presumed interneuron. Images represent several averaged z-planes totaling < 3 μm. Scale bars, 10 μm. **d)** Single-cell RT-PCR reveals that large fastigial GFP– neurons express the glutamatergic marker VGluT2, while GFP+ neurons express GlyT2. Right, whole-brain RNA processed alongside experimental samples. Lowest ladder band is 200 bp, increments of 100 bp. Performed as in Bagnall et al., 2007.

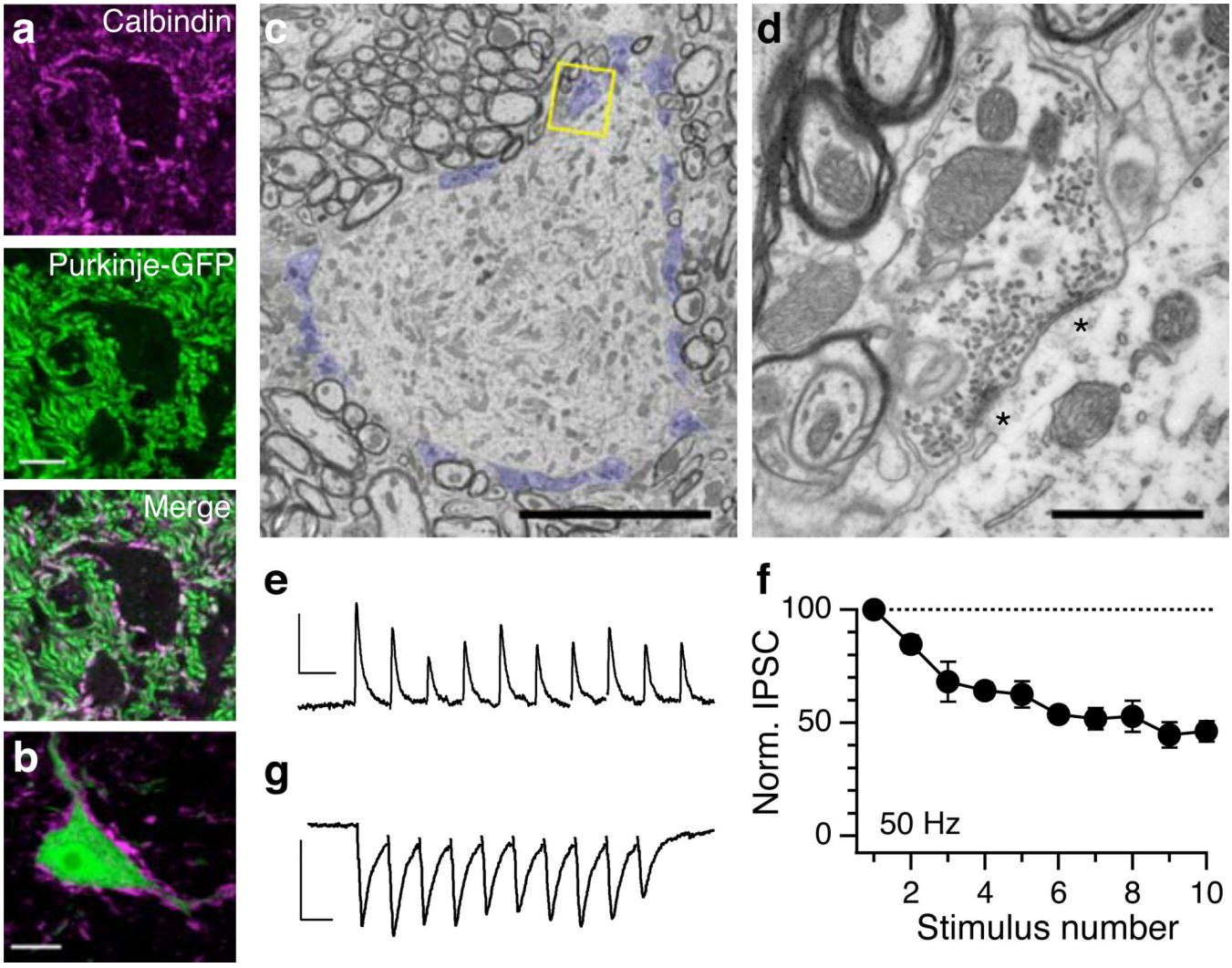

Figure 2. Purkinje cells inhibit large fastigial glycinergic neurons

a) Calbindin immunostaining (top) identifies Purkinje cell terminals, visualized in the L7-GFP mouse (center) (Sekirnjak et al., 2003). Scale bar, 10 μm. **b)** Calbindin immunostaining (magenta) in the GlyT2-GFP line reveals that large fastigial glycinergic neurons are surrounded by Purkinje cell terminals. All confocal images represent 1–6 averaged z-sections (< 3 μm total). **c)** Electron micrograph of a large glycinergic neuron showing many Purkinje cell synapses (blue) on soma. Scale bar, 10 μm. **d)** Higher magnification view of the synapse outlined in c with two release sites (asterisks) displaying typical Purkinje cell features: large bouton size, symmetric synaptic density, and elliptical vesicles. Scale bar, 1 μm. **e)** White matter stimulation during whole-cell recording of large glycinergic fastigial neuron elicits a gabazine-sensitive synaptic current. Stimulus artifacts blanked for clarity. Scale bars, 100 pA, 20 ms. **f)** GABAergic currents exhibit sustained transmission at 50 Hz (n = 4; mean ± s.e.m.). **g)** Glutamatergic synaptic currents (DNQX- and CPP-sensitive) recorded in another large glycinergic fastigial neuron. Scale bars, 100 pA, 20 ms.

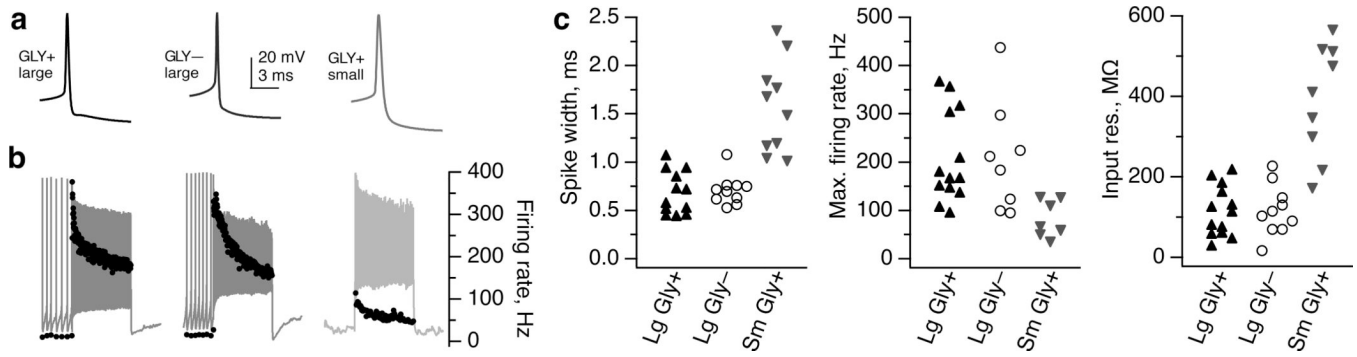

Figure 3. Physiological characteristics of large fastigial glycinergic neurons resemble those of large glutamatergic neurons, not small glycinergic neurons

a) Action potential waveforms recorded from a typical large glycinergic neuron (left), large glutamatergic neuron (center), and small glycinergic neuron (right). **b)** Response to a 1 s step of depolarizing current at the maximum level to which the neuron could fire continuously across the whole step. Right axis, instantaneous firing rate. **c)** Small glycinergic neurons are significantly different from both large glutamatergic and large glycinergic neurons in action potential width (left), maximum firing rate (middle), and input resistance (right) ($p < 0.05$, Wilcoxon unpaired t-test, for all small vs. large comparisons), while large glutamatergic and glycinergic neurons did not differ significantly ($p > 0.3$, all large glycinergic vs large glutamatergic comparisons).

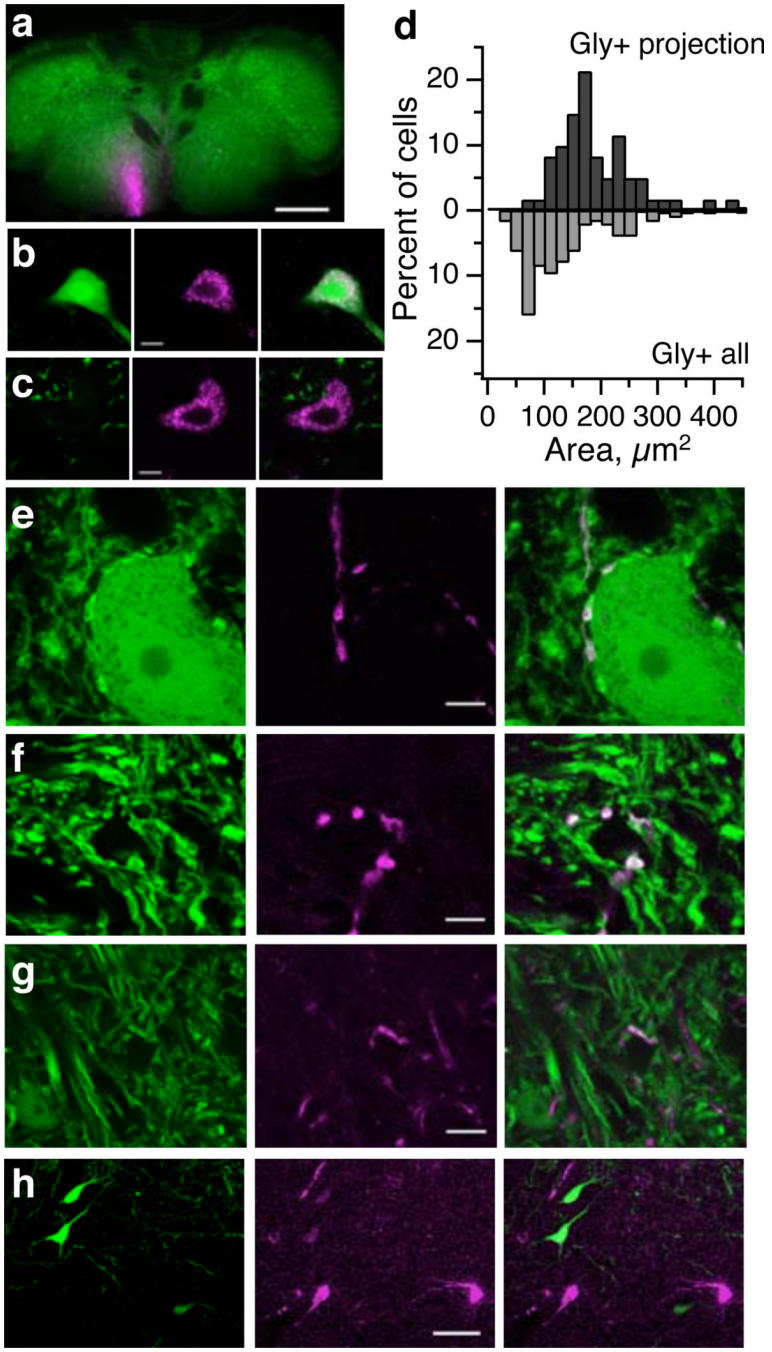

Figure 4. Glycinergic fastigial neurons project to the ipsilateral brainstem, while glutamatergic neurons project contralaterally

a) Injection site in caudal medulla. Scale bar, 500 μm. **b)** Ipsilateral to injection, retrogradely labeled fastigial neurons are glycinergic (GFP+). In this and subsequent images: left, GFP expression; middle, retrograde labelling; right, merge; scale bar 10 μm. **c)** Contralateral to injection, retrogradely labeled fastigial neurons are glutamatergic. **d)** Histogram distribution of somatic area of retrogradely labeled Gly+ cells (top, n = 61 neurons from several animals) versus all Gly+ deep nuclear neurons (bottom, n = 132 neurons). **e)** Anterogradely labeled glycinergic fastigial axons synapse onto glycinergic and **f)** non-glycinergic neurons in the ventromedial medullary reticular formation. **g)** Axonal

swellings from glycinergic fastigial projections are also seen in the vestibular nuclei (here, the spinal vestibular nucleus). **h)** No glycinergic retrogradely labeled neurons were seen following tracer injections to the thalamus.

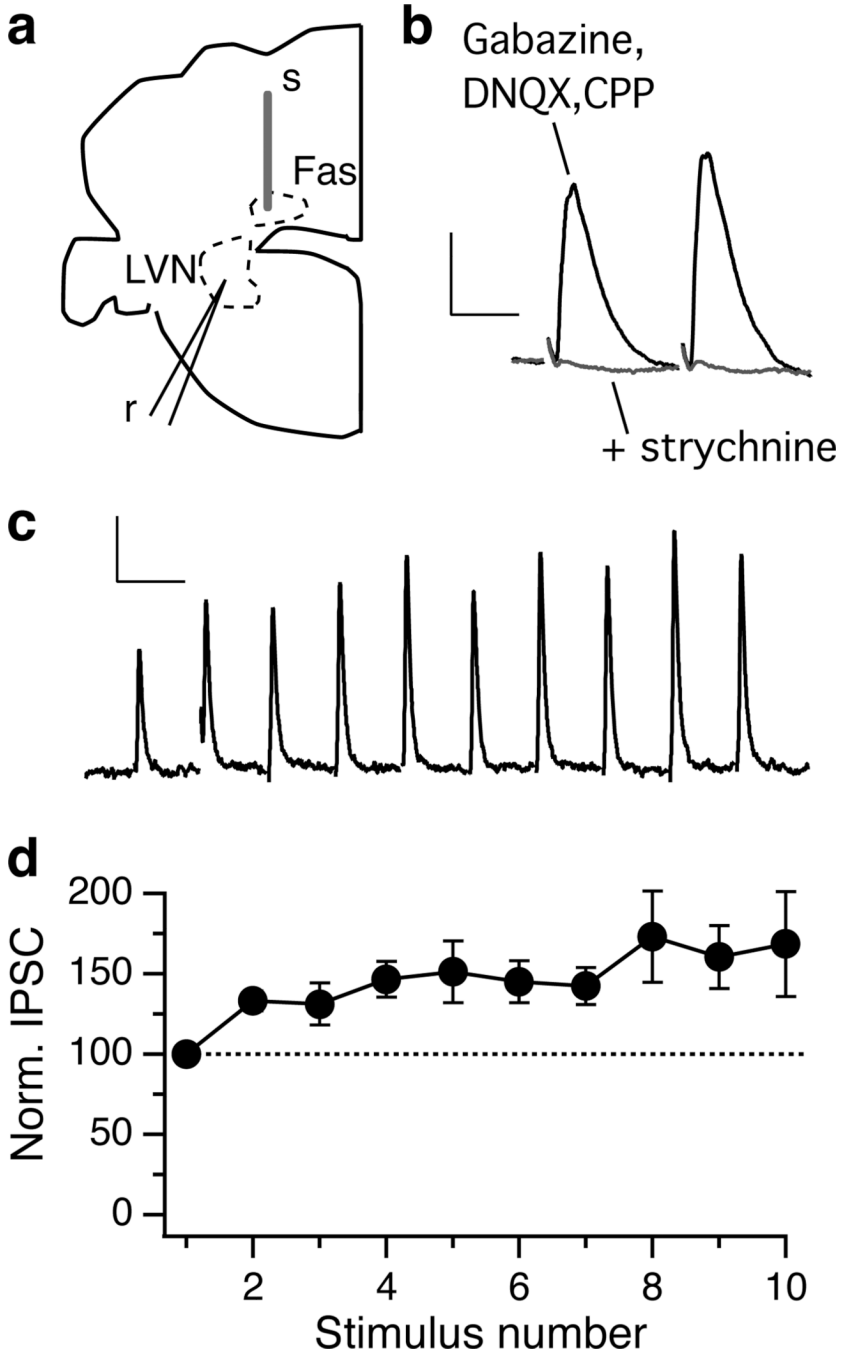

Figure 5. Functional inhibitory projection from the fastigial nucleus to the brainstem

a) Diagram of the recording setup. Left half of a coronal section; top is dorsal, right is medial. A concentric bipolar stimulating electrode (s) was placed in the fastigial nucleus (Fas), and whole-cell recordings (r) were made in the lateral vestibular nucleus (LVN). **b)** The outward synaptic currents recorded in an LVN neuron in the presence of ionotropic GABAergic and glutamatergic antagonists is abolished by application of strychine (1 μm) Scale bars, 100 pA, 10 ms. Stimulus artifacts have been blanked. **c)** Response to a stimulus train at 50 Hz in another LVN neuron. The subtracted strychnine-sensitive component is shown. Scale bars, 100 pA, 20 ms. **d)** Fastigial glycinergic currents facilitated during a train of 10 stimuli delivered at 50 Hz (n = 5; mean ± s.e.m.).